Comparison of Image Quality between Energy Integrating and Photon Counting CT for Prostate Artery Embolisation Planning

Angus Scott Fraser[1, 2, a)], Michael Barnard[1], Robert Wise[1], Benjamin JR Kemp[1], David J Platten[3], Kawal S Rhode[2]

[1]Oxford University Hospitals NHS Foundation Trust

[2]School of Biomedical Engineering and Imaging Sciences, King's College London

[3]Radiation Protection, United Lincolnshire Hospitals NHS Trust

[a)]Corresponding author: Mr Angus Scott Fraser; Angus.Fraser@ouh.nhs.uk

Prostate Artery Embolisation (PAE)

- Treatment for benign prostate hyperplasia, i.e., enlarged prostate by blocking its blood supply
- Less invasive alternative to surgical resection, potentially even as an outpatient procedure
- Demands a highly skilled operator due to the nature of the anatomy, e.g., highly varied origin of prostatic artery
- PAE is always guided with intraprocedural fluoroscopy and CBCT, but a pre-procedural CTA can be used for planning
  - This is associated with significant reductions in screening and procedure time[2]

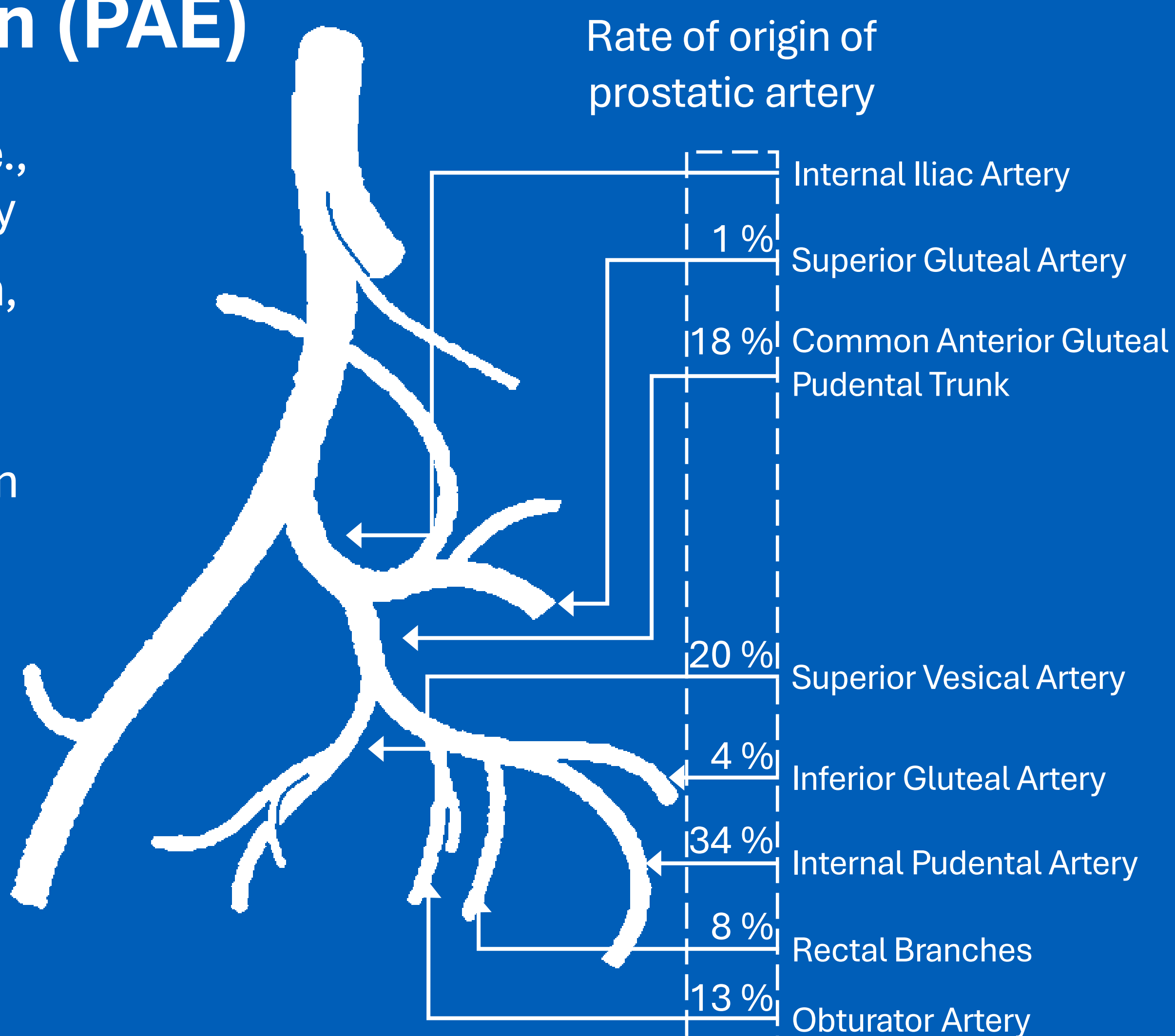

Figure 1: Internal Iliac Artery vascular anatomy[1]

PAE Planning CTA - Challenges

- There are numerous challenges with PAE Planning CTAs too:
  - Vasculature
    - Small, average diameter 0.5-1.5 mm[1]
    - Very tortuous
    - Highly varied origin
    - High incidence of anastomoses
  - Common comorbidities
    - Obesity
    - Atherosclerosis
    - Calcifications
- Current energy-integrating CT (EI-CT) is pushed to, if not beyond, its technical limits in this application

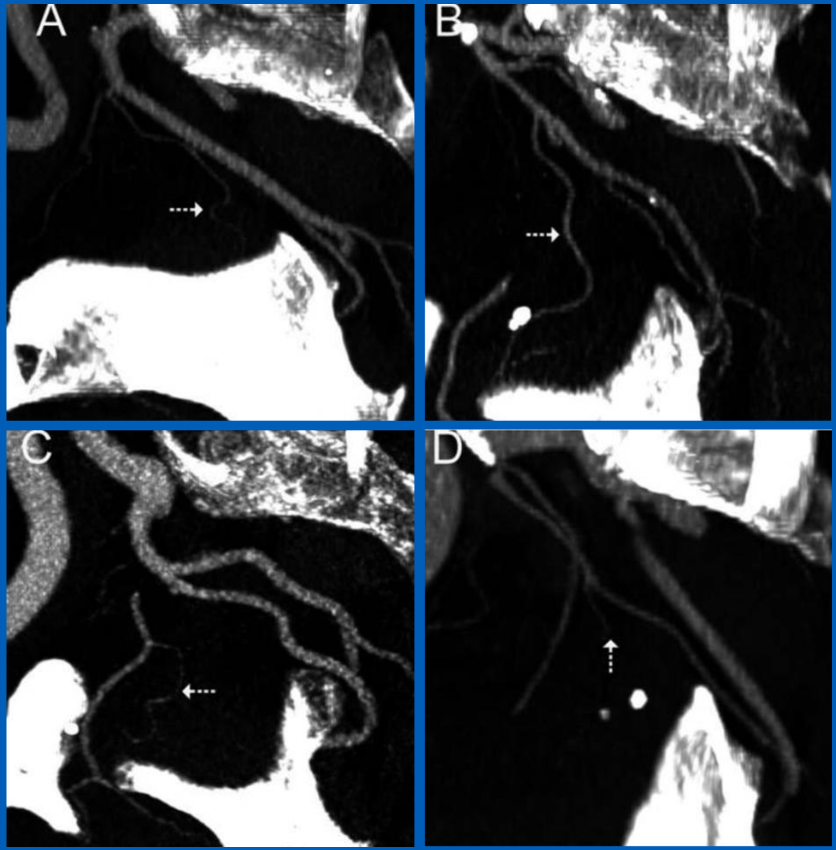

Figure 2: CTA MIP images of prostatic artery with varied origins[3]

PAE Planning CTA - Solutions

- Photon counting CT (PC-CT) seems uniquely well suited to these challenges due to:

Figure 3: Siemens NAEOTOM Alpha Photon Counting CT[4]

PC-CT – Spatial Resolution

- Photon counting CT (PC-CT) seems uniquely well suited to these challenges due to:
  - No need for septa between detector elements
    - Smaller pixels, improved spatial resolution

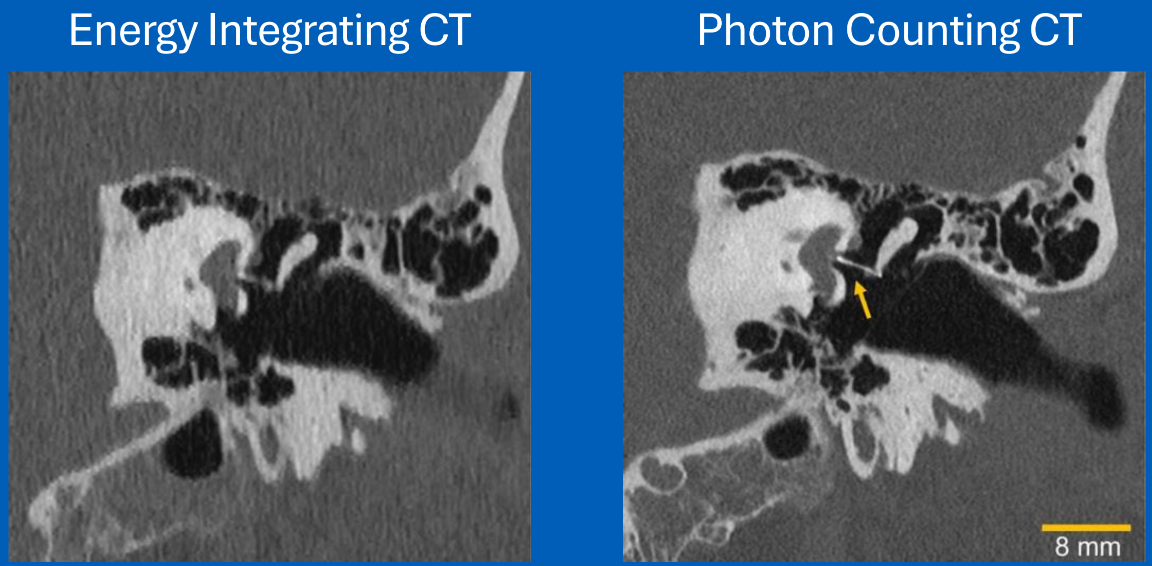

Figure 4: Sub-mm metal prosthesis in inner ear[5]

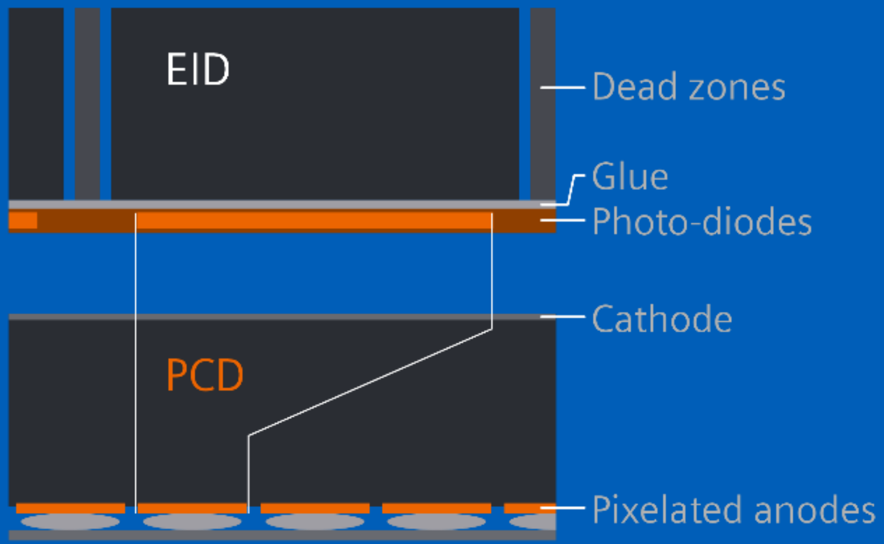

Figure 5: Relative sizes of PC-CT and EI-CT detector elements. Provided by Siemens Healthineers

PC-CT – Signal & Noise

- Photon counting CT (PC-CT) seems uniquely well suited to these challenges due to:
  - No need for septa between detector elements
    - Smaller pixels, improved spatial resolution
  - Signal independent of photon energy
    - Equal weight to low-keV photons significantly mitigates beam hardening

Energy Integrating CT   Photon Counting CT

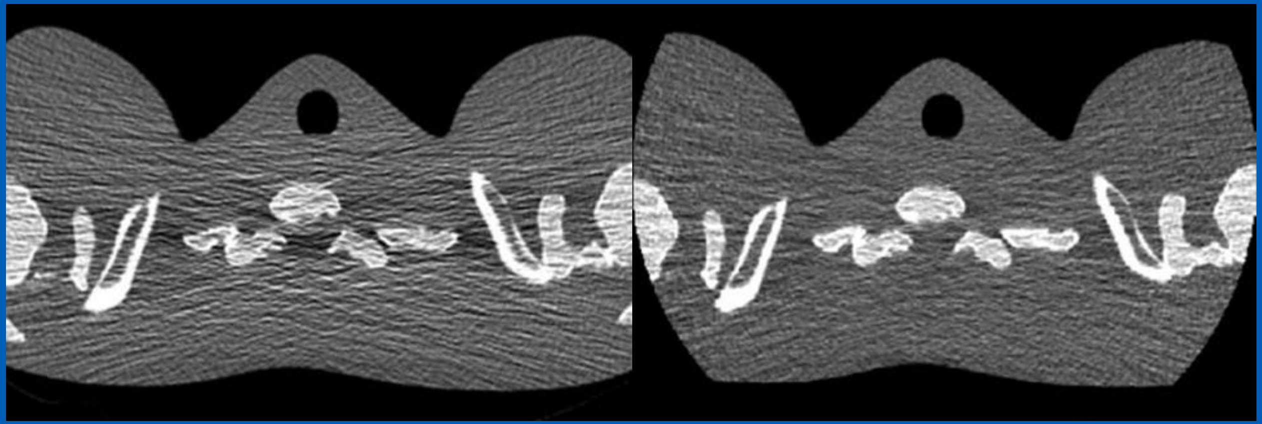

Figure 6: Large anthropomorphic phantom images with 120 mAs for both systems[6]

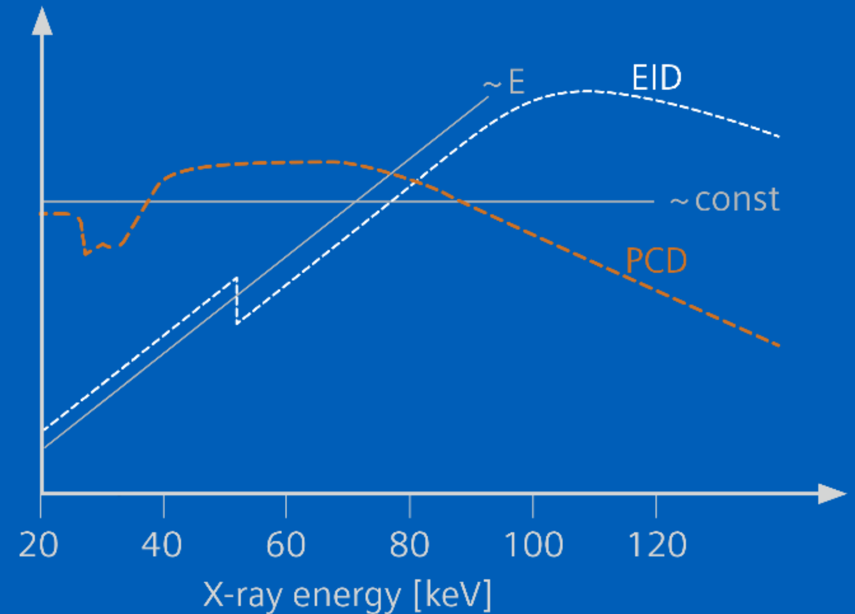

Figure 7: Detector responsivity [a.u] with photon energy. Provided by Siemens Healthineers

PC-CT – Spectral Sensitivity

- Photon counting CT (PC-CT) seems uniquely well suited to these challenges due to:
  - No need for septa between detector elements
    - Smaller pixels possible
      - Improves spatial resolution
  - Signal independent of photon energy
    - More contrast information carried by low-keV photons
      - Significant mitigation of beam hardening
  - Individual pulse processing
    - Apply threshold to eliminate electronic noise
    - Spectral data with every acquisition

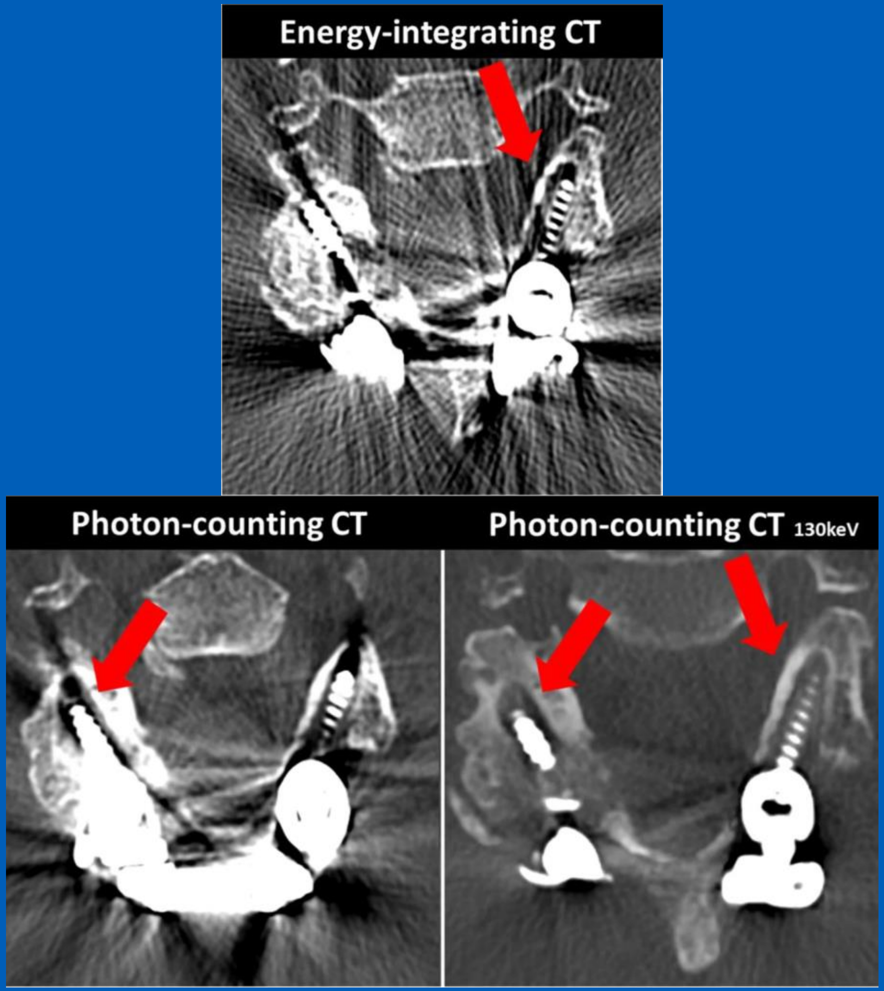

Figure 8: Images of metal screw implant in spinal disk[7]

Image Quality Assessment - Methods

- From AAPM Task Group 233, d' is a performance metric comprising of[8]:
  - A clinical task to be performed, on images produced by a given system
    - This accounts for the system's noise performance
  - An observer based on a mathematical model of the eye's frequency response for images on a display under assumed ambient lighting
  - Clinical image(s) to be assessed, i.e., to act as a source for the real clinical task
- Well suited to tasks based on contrast threshold detectability

$$d' = \frac{\int_0^{f_N} |W(f)|^2 \cdot TTF^2(f) \cdot E^2(f)\, df}{\sqrt{\int_0^{f_N} |W(f)|^2 \cdot TTF^2(f) \cdot NPS(f) \cdot E^4(f)\, df}}$$

- *d'* = Detectability index, essentially a score for a system's response to a given signal
- *W(f)* = Task function, a 'perfect' version of the signal to be detected on clinical images
- *TTF(f)* = Task transfer function is based on the system's response to a standardised, scaled up feature of the same shape, composition and contrast as modelled by W(f)
  - Analogous to MTF, but for a specific task
- *E(f)* = 'Eye model', i.e., the frequency response of the observer
- *NPS(f)* = Noise Power Spectrum, describes the noise and its texture in the image
- f = radial spatial frequency, f_N = Image pixel Nyquist frequency

Note: Equation adapted to assume radially symmetric task function[9]

Image Quality Assessment - Materials

- Using a Sun Nuclear Mercury 4.0 phantoms
  - 5 tiers, each containing a 30 mm uniformity and material insert section
- NPS and TTF measured over central 15 mm in each section using David Platten's Quantitative IQA plugin for ImageJ
- Results were then used to calculate d' for a range of task diameters representative of the prostatic artery

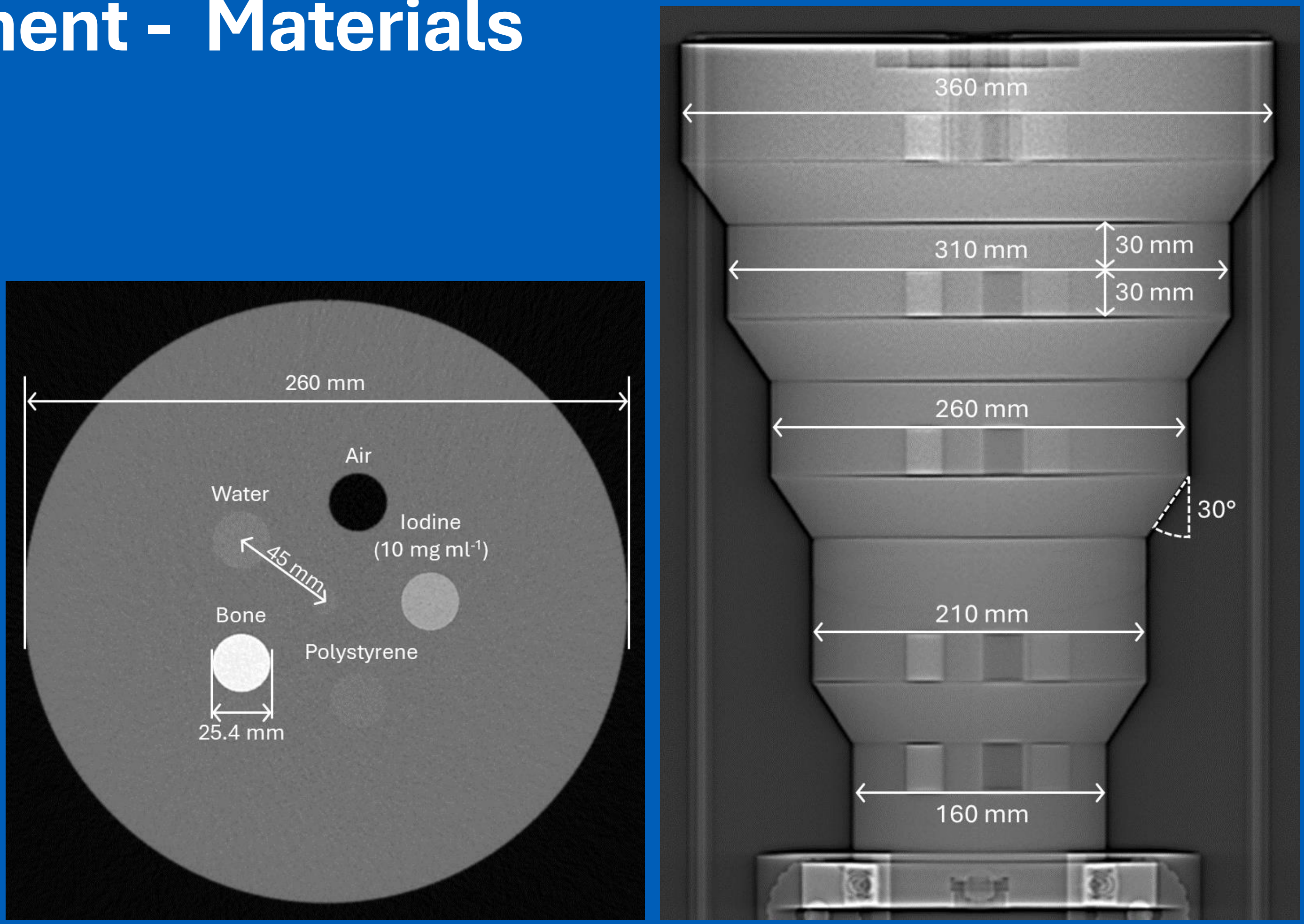

Figure 9: Material inserts in 26 cm section of phantom (left) and topogram showing phantom dimensions (right)

CT Systems and Protocols

Parameter	EI-CT		PC-CT	
Manufacturer - Model	GE Healthcare – Revolution CT		Siemens Healthineers – NAEOTOM Alpha	
Protocol	PAE Planning	PAE Planning (GSI)	PAE Planning	
Tube voltage [kV]	100	140/80	120	
Tube current modulation	On	Off (320 mA)	On	
Detector collimation	128 × 0.625 mm (80 mm)		120 × 0.2 mm (24 mm)	
Pitch	0.992		0.85	
Image Quality Index	Noise Index = 22.0		CARE keV level = 117 keV	
Reconstruction Kernel and algorithm	SOFT ASiR – 50%	STANDARD ASiR – 60%	Bv44u (Conventional) QIR – 3	Qr44v (Spectral) QIR – 3
Image Types Being Assessed	Conventional	VMI (50, 58 & 70 keV) Iodine Map	Conventional	VMI (50, 58 & 70 keV) Iodine Map
Imaged slice width [mm]	0.625		0.2	0.4
Matrix size	512		1024	512 (VMI Only)
$CTDI_{vol}$ (32 cm) [mGy]	5.09	7.95	5.01	

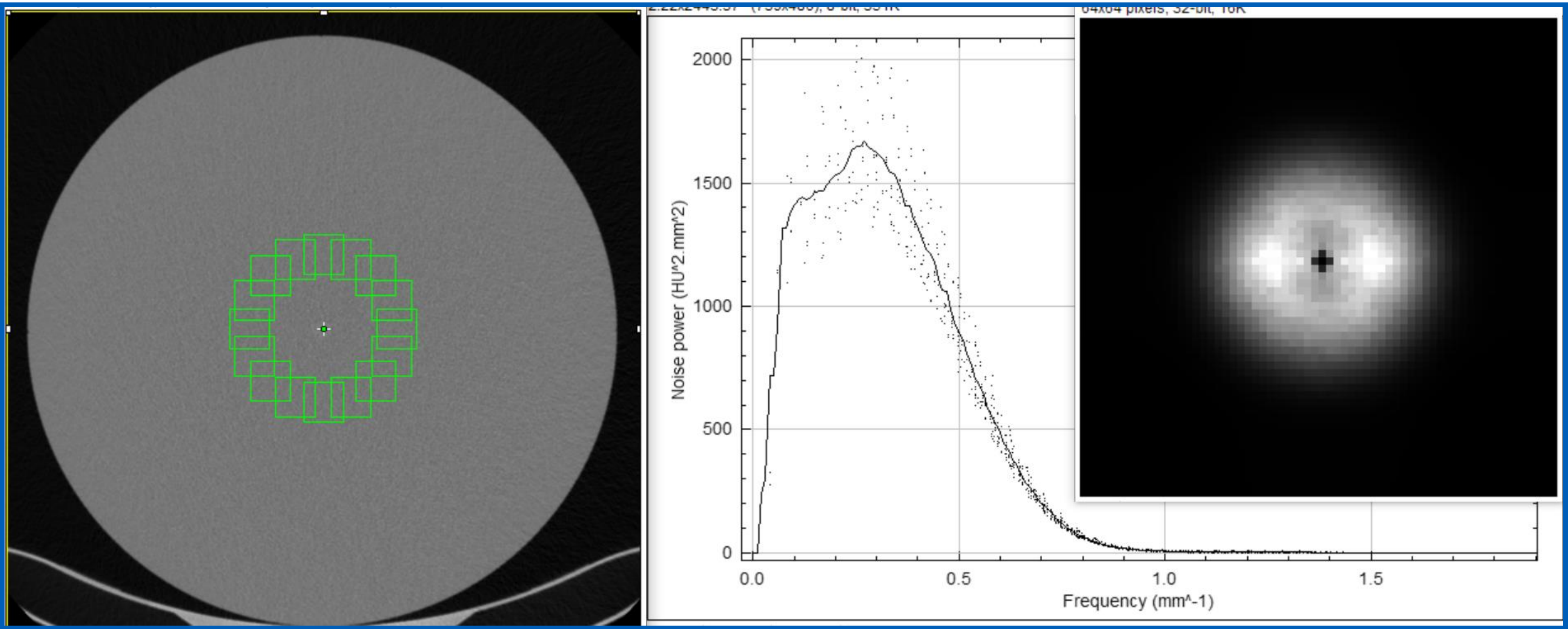

Noise Power Spectrum

CT – Image Type	PC-CT – 120 kV_p Conventional
Phantom diameter	360 mm
Voxel size (mm)	0.377 x 0.377 x 0.2
Slices measured	76 (15.2 mm)
No., size of records	16, 64 x 64

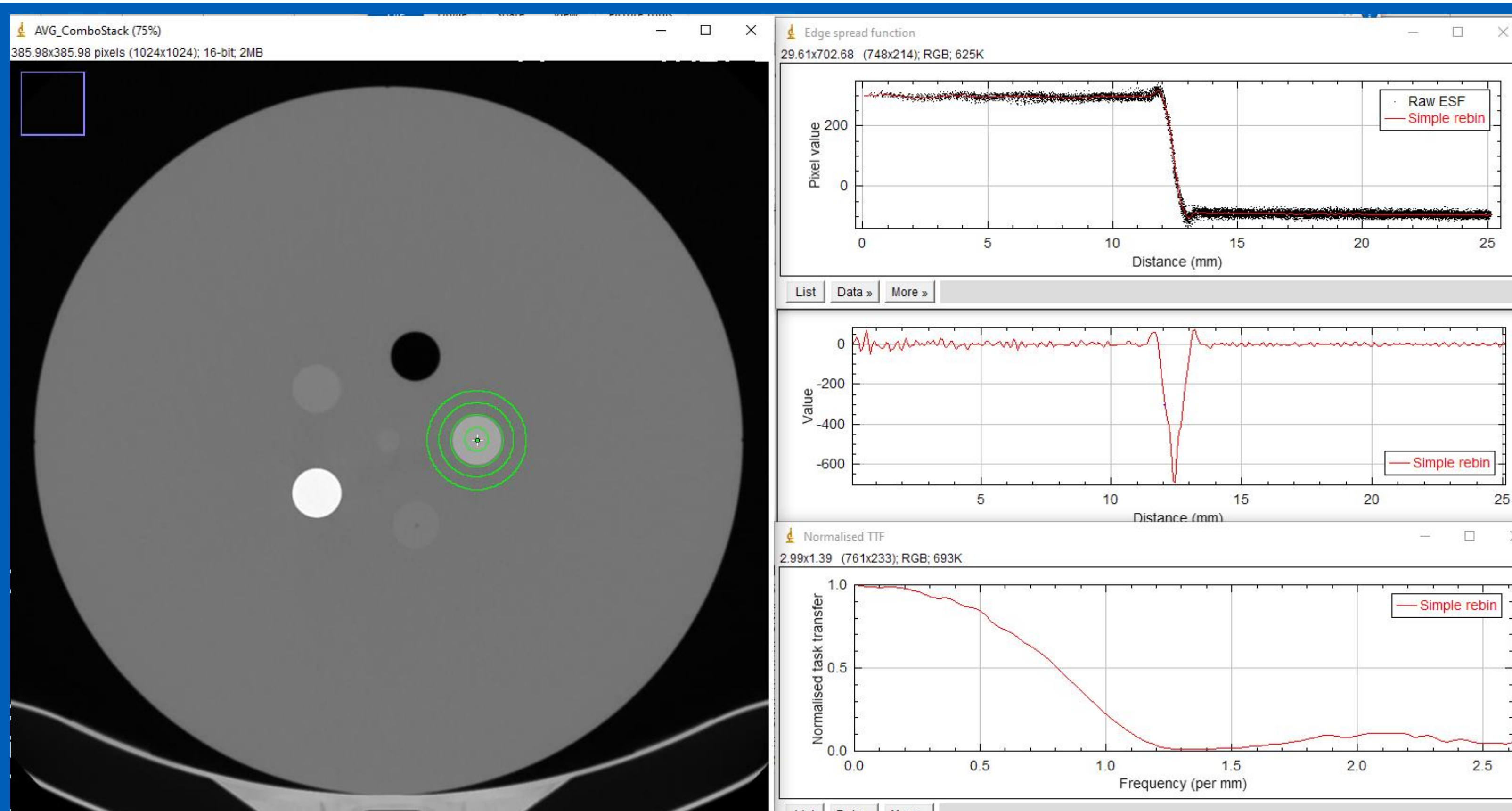

Task Transfer Function – Iodine

CT – Image Type	PC-CT – 120 kV_p Conventional
Phantom diameter	360 mm
Voxel size (mm)	0.377 x 0.377 x 0.2
Slices measured	76 (15.2 mm)

Results – NPS & TTF

- NPS
    - $CTDI_{vol}$ almost matched for conventional images, but ISW for EI-CT is ~3x that of PC-CT
    - EI-CT's low energy spectrum weighting in VMI reconstruction will not change despite disproportionate attenuation
- CNR
    - PC-CT aims to maintain CNR, hence its stability here
- TTF
    - PC-CT conventional images reconstructed with 1024x1024 matrix Vs 512x512 for the rest

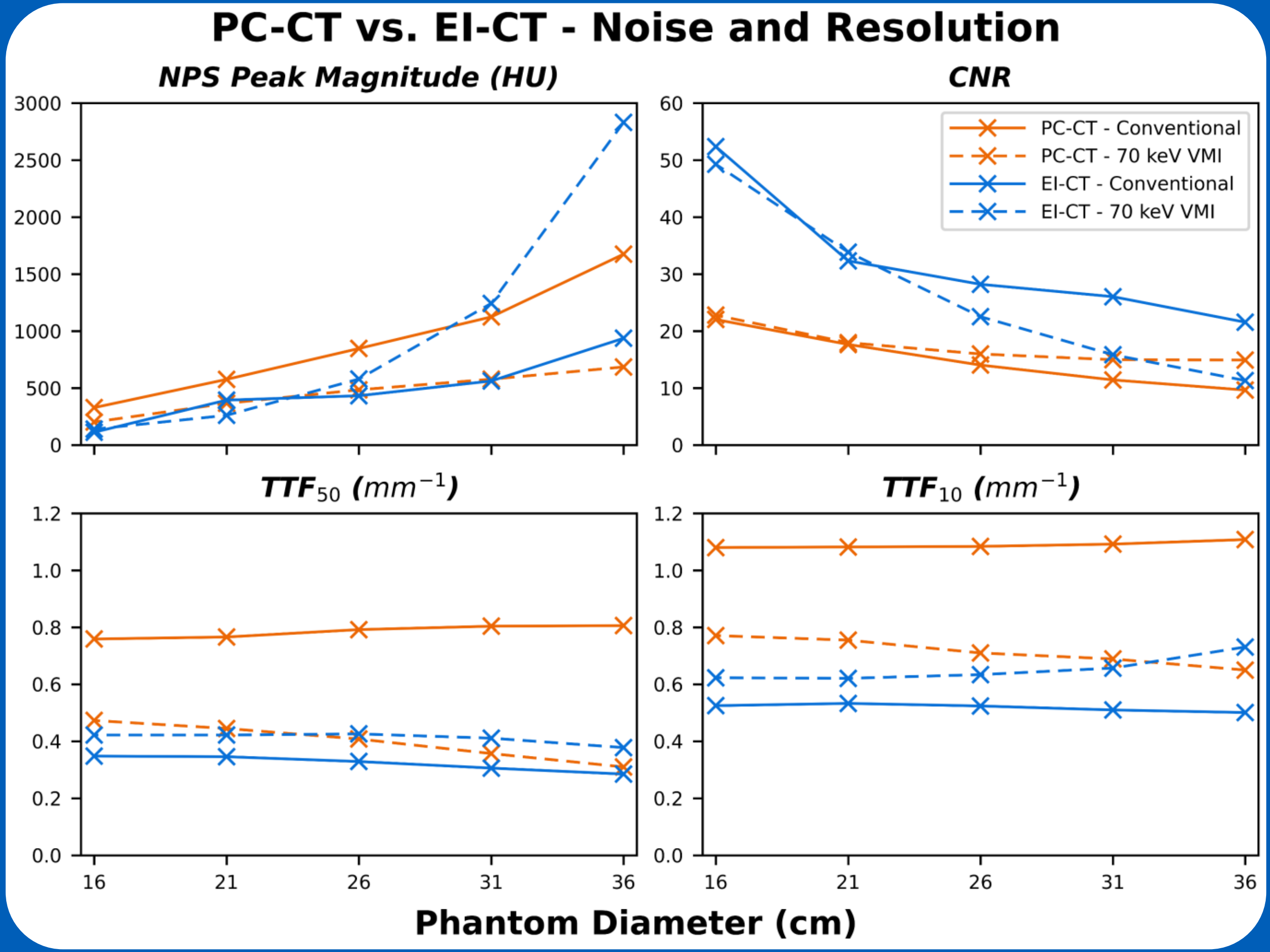

Figure 5: Noise Power Spectrum and Task Transfer Function Results

Results – d'

- Conventional
  - PC-CT outperformed for task diameters of 0.5 and 1.0 mm
  - Also outperformed to a lesser degree for phantom diameter of 21 cm
- 70 keV VMI
  - Relative performance strongly dependent on phantom diameter
- Should the PC-CT have performed better?

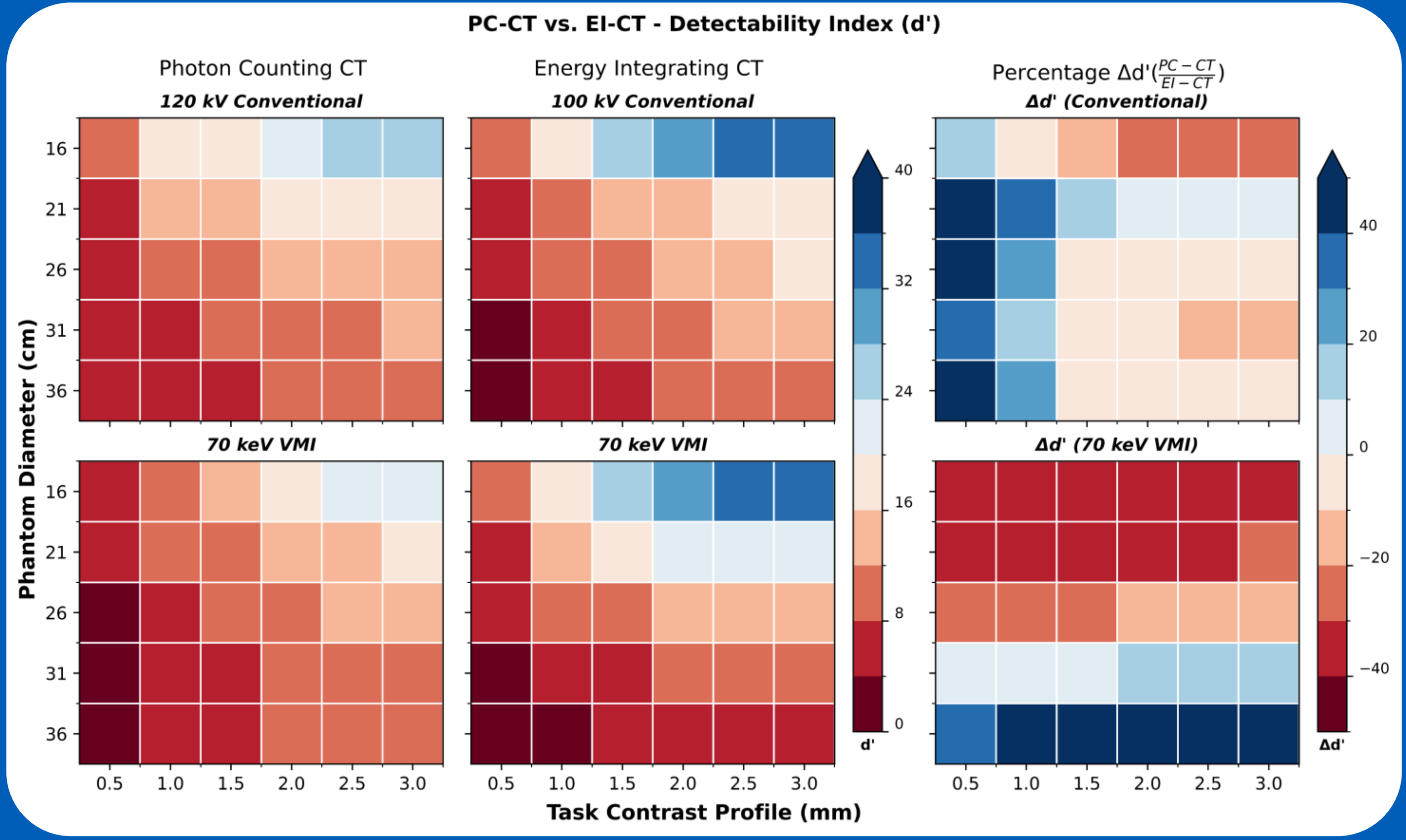

Figure 7: Detectability index results. Absolute values for conventional and 70 keV VMI images (left, centre) and percentage difference (right). Blue = better for PC-CT.

Discussion

- Conventional
  - 0.5 mm and 1.0 mm task diameters
    - Nyquist limit for detector pixels is 1.25 mm for the EI-CT, 0.4 mm for the PC-CT
    - PC-CT image pixel spacing was approx. half that of the EI-CT due to the latter using a larger image matrix.
  - 21 cm phantom diameter
    - Only section in phantom where current was higher for the PC-CT
- 70 keV VMI
  - No tube current modulation for the EI-CT, effective 320 mA
  - Image pixel spacing was approximately equal for both systems
  - 36 cm phantom diameter
    - PC-CT signal dependence on quantity of photons better preserves low-energy signal following degradation due to beam hardening[6]

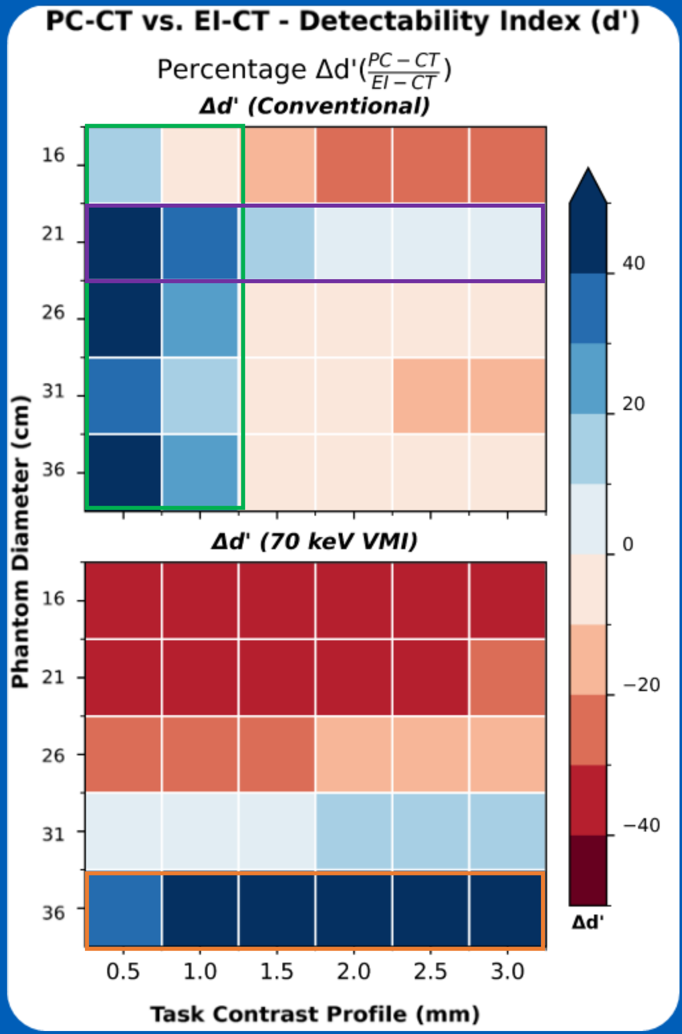

Figure 7: Detectability index results (Percentage difference only). Blue = better for PC-CT.

Conclusions and Further Work

- Results are representative of OUH clinical protocols for PAE planning
- Findings should not be used to judge the performance of the systems themselves
- PC-CT performing better for task diameters representative of the prostatic artery in conventional images may well explain why it is preferred by clinicians carrying out PAE procedures despite performing worse in most conditions modelled thus far
- Data acquired under varied exposure conditions (e.g., lower VMI energies, include iodine maps etc.) have been acquired and are under review

References

1. Cornelis F, Bilhim T, Hacking N, Sapoval M, Tapping C, Carnevale F. CIRSE Standards of Practice on Prostatic Artery Embolisation. *Cardiovascular and interventional radiology*. 12/02 2019;43doi:10.1007/s00270-019-02379-3

2. Steiniger B, Fiebich M, Grimm M-O, et al. PAE planning: Radiation exposure and image quality of CT and CBCT. *European Journal of Radiology*. 2024/03/01/ 2024;172:111329. doi: https://doi.org/10.1016/j.ejrad.2024.111329

3. Moschouris H, Stamatiou K, Tzamarias S, et al. Angiographic Imaging of Prostatic Artery Origin in a Greek Population and Correlation With Technical and Clinical Aspects of Prostatic Artery Embolization. *Cureus*. 2023;doi:10.7759/cureus.45941

4. Siemens. Siemens Naeotom Alpha Photo - Face On. In: siemens-healthineers_CT_NAEOTOM-Alpha, editor.: Siemens Medical Solutions USA; 2022.

5. McCollough, C. H., Rajendran, K., & Leng, S. (2023). Standardization and Quantitative Imaging With Photon-Counting Detector CT. Invest Radiol, 58(7), 451-458. https://doi.org/10.1097/rli.0000000000000948

6. Yu Z, Leng S, Kappler S, et al. Noise performance of low-dose CT: comparison between an energy integrating detector and a photon counting detector using a whole-body research photon counting CT scanner. Journal of Medical Imaging. 2016;3(4):043503.

7. Rau, A., Straehle, J., Stein, T., Diallo, T., Rau, S., Faby, S., Nikolaou, K., Schoenberg, S. O., Overhoff, D., Beck, J., Urbach, H., Klingler, J.-H., Bamberg, F., & Weiss, J. (2023). Photon-Counting Computed Tomography (PC-CT) of the spine: impact on diagnostic confidence and radiation dose. European Radiology, 33(8), 5578-5586. https://doi.org/10.1007/s00330-023-09511-5

8. Ehsan Samei DB, Kirsten L Boedeker, Samuel Brady, Jiahua Fan, Shuai Leng, Kyle J. Myers, Lucretiu M. Popescu, Juan Carlos Ramirez Giraldo, Frank Ranallo, Justin Solomon, Jay Vaishnav, and Jia Wang. *Task Group No. 233 - Performance Evaluation of Computed Tomography Systems (TG233)*. 2019.

9. Solomon J, Wilson J, Samei E. Characteristic image quality of a third generation dual-source MDCT scanner: Noise, resolution, and detectability. *Med Phys*. Aug 2015;42(8):4941-53. doi:10.1118/1.4923172

Disclosures & Acknowledgements

No relevant financial relationships or conflicts of interest exist

The work presented has been classified as a service evaluation

The Siemens NAEOTOM Alpha used in this study is owned and operated by the University of Oxford, and MPE services for its use are provided by a third party